

A NEW DAMAGE INDICATOR IN TIME AND FREQUENCY DOMAINS FOR STRUCTURAL HEALTH MONITORING: THE CASE OF BEAM WITH A BREATHING CRACK

FERGYANTO EFENDY GUNAWAN

Industrial Engineering Department, BINUS Graduate Program – Master of Industrial Engineering
Bina Nusantara University

Jl. K. H. Syahdan No. 9, Kemanggisian, Palmerah, Jakarta 11480, Indonesia
fgunawan@binus.edu

Received April 2020; revised August 2020

ABSTRACT. *With the adoption of the damage tolerance design principle, the health monitoring system has become an integral part of the operation of engineering structures. For the system to work, a damage indicator that describes the structural integrity level should be established and monitored. The damage indicator is usually derived from structural responses. Many quantities have been proposed for damage indicator including natural frequency, mode shape, curvature, strain energy, and t -, F -, and z -statistics. In this paper, we propose a new damage indicator in the time and frequency domains derived from the Euler-Bernoulli beam theory. We evaluate the method by using data obtained from a numerical simulation of a cracked beam. The beam deformation is nonlinear due to the contact between the crack faces during vibration. The proposed damage index is estimated in the domains for various observation points on the beam. Besides, the existence of the crack is also predicted by the widely used traditional method based on the change of the natural frequency and mode shape. A comparison is made between the present method and the existing ones. We conclude the present proposal is more sensitive to detect the crack.*

Keywords: Euler-Bernoulli beam, Structural health monitoring, Damage indicator, Natural frequency, Finite element method

1. Introduction. Structural Health Monitoring (SHM) is a system integrating many subsystems including a subsystem of sensors and data acquisition, a subsystem of information and communication technology, a database subsystem, and a structural management subsystem. The system is essential to provide the guarantee of safe and reliable operation of engineering systems. It allows us to monitor the integrity of engineering structures in real time; hence, the potentially catastrophic failures can be avoided. The use of the SHM system has been evaluated for various engineering structures including bridges [1–7] and airplanes [8–11]. Those required subsystems are interrelated to set up a complete SHM system as illustrated in Figure 1 [12]. The component that labeled ‘On-bridge’ can be considered to be for any engineering structure of interest.

In general, the SHM system works by relating structural deformation data, structural integrity, and machine learning algorithms. Features derived from structural deformation data are crucial for the system to assess structural integrity. So far, the most popular features are the structural natural frequencies and mode shapes [5,13–18]. Those features can simply be reduced from the deformation data. Those indicators are useful despite their limitations. Natural frequency and mode shape are good indicators. Natural frequency is global as damage at any point on a structure affects the indicator. However, when small

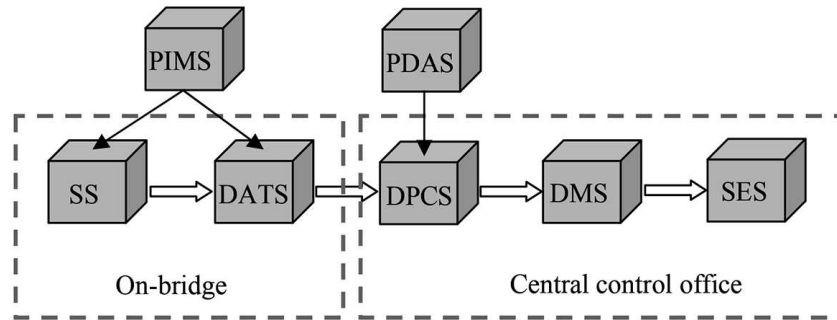


FIGURE 1. The architecture of structural health monitoring system: PIMS = Portable Inspection and Maintenance Subsystem; SS = Sensor Subsystem; DATS = Data Acquisition and Transmission Subsystem; PDAS = Portable Data Acquisition System; DPCS = Data Processing and Control Subsystem; DMS = Data Management Subsystem; SES = Structural Evaluation Subsystem [12]

damage instantiates, natural frequency often only changes slightly, hardly detectable. Mode shape is also global, but the measurement at several points is required to establish the indicator. Vibration curvature and elastic energy possess similar characteristics. The power spectral density can hardly differentiate the healthy condition from the damaged condition when the damage level is small as pointed out by [19].

The flow of information and assessment of the structural integrity occurs with the following sequence. The flow is all started from the sensor subsystem, labeled with SS. Generally, the subsystem consists of sensors for structural responses such as strain, acceleration, or displacement. The information is acquired and recorded temporarily by the Data Acquisition and Transmission Subsystem (DATS). An additional system called Portable Inspection and Maintenance Subsystem (PIMS) may also be incorporated.

The second major component is labeled ‘Central Control Office’, consisting of subsystems of Data Processing and Control Subsystem (DPCS), Data Management Subsystem (DMS), and Structural Evaluation Subsystem (SES). The latter subsystem is one of the most critical subsystems that translates the structural response data to structural integrity level, and damage location and level. The subsystem reduces the response data into features that are sensitive to structural damages for both location and level.

As for the damage sensitive features, many research papers have considered the structural natural frequencies and mode shapes [5, 13–18]. Many recent publications proposed machine learning techniques for SHM [9, 10, 20–27]. Also, the structural curvature, elastic energy, and power spectral density during vibration are widely used. Although each feature has its benefits and limitations, it is generally accepted that the detection is only possible when the damage has reached a certain level [19]. Lately, many machine learning techniques have been evaluated for SHM applications [9, 10, 20–27]. However, two major journals in the field, *Journal of Mechanical Systems and Signal Processing* and *Journal of Sound and Vibration*, put forward the remarks regarding the trend. They consider that applying machine learning only to solving mechanical system problems without applying sound engineering principles is insufficient to justify publication.

The methods proposed for damage detection by each of the above references are briefly and concisely described as the following. [13] proposed a 3-layer Artificial Neural Network (ANN) model with inputting a vector consisting of the structural natural frequencies and mode shapes and outputting a vector consisting of damage severities on structural joints. [5] proposed a clustering method where the damage sensitive features were the

impulse response function projected to a few dominant eigenvectors. The vectors were obtained from the covariance matrix of the impulse response function. [14] proposed the COordinate Modal Assurance Criterion (COMAC) and modal strain energy. [15] proposed the change of the Frequency Response Functions (FRF) between two states: healthy and damaged. The change was measured by the difference and correlation of FRFs. [16] and [17] proposed the use of the wavelet transform on the structural response data. [18] and [19] proposed the use of the Power Spectral Density (PSD). [20] proposed a back-propagation feed-forward neural network to predict the crack length on a lap joint based on inputs of the strains at many measurement points. The strains were approximated with the first 20 terms of the Fourier series. Furthermore, the Fourier coefficients were reduced into six principal components, which were used as the input vector of the ANN model. [21] proposed ANN models in the hierarchy for crack characterization and its location. [22] addressed the problem in [21] by using support vector machine.

In our perspective, machine learning techniques are applicable when a large size dataset is available. For SHM, where structural data in healthy and damaged conditions are required, the existing data are usually limited. Those who proposed machine learning techniques were using data from engineering simulations that often require many assumptions and do not entirely resemble the actual engineering structures.

A new and better indicator is required. It should be more sensitive to damage, require a minimum amount of data, and be easily measured. This paper addresses those issues. In this work, we propose a new damage sensitive index in the time and frequency domains. We derive the feature from the structural governing dynamics and are expected to be more sensitive to damage than the existing technique. Traditionally, in the design phase of engineering structures, the structural governing dynamics are only utilized to estimate deformation and stress, making sure structures can be operated safely. In operation, the governing dynamics are being used to estimate the loads subjected to the structures, making sure that structures are not subjected beyond their critical loads. Thus, this paper offers a new application of the structural governing dynamics that is for monitoring of structural integrity. In this paper, we demonstrate the index by analyzing a cracked beam specimen and compare the results with that by using the natural frequency method. The method is evaluated on a beam structure with a breathing crack. The problem is more complex because the structural responses may be nonlinear due to the potential interaction between the crack faces during vibration. The index was evaluated on a Euler-Bernoulli beam with damage smeared uniformly in the structure in [28] and on an idealized system in [29].

It proposes an indicator developed based on our understanding of the theory regarding the strength of materials. An initial assessment of the method applied to a spring-mass system is presented in [29].

We structure the paper as the following. Section 2, Research Method, describes the derivation of the damage indicator and the method to generate sample data where the indicator is empirically evaluated. Section 3, Results and Discussion, presents the results of the computed damage indicator. In this section, we also compare with the results of natural frequency method. Finally, in Section 4, Conclusion, we conclude the most essential aspects contributed by this research.

2. Research Method. By this paper, we wish to propose a new damage indicator for structural health monitoring that is derived from our understanding of the structural dynamics in intact condition. We limit our discussion to the case of a two-dimensional beam structure. However, we believe the idea is generally applicable to the engineering structure in general. We have assessed the idea of using the governing dynamics of the

structure for monitoring the structure condition in a few engineering cases. In [29, 30], we evaluated the index in an idealized condition where the engineering structure was simplified as a system of a set of springs and masses. In [28, 31], we evaluated the index for monitoring damage in a beam structural member where the damage was considered occurring uniformly across a beam section. The present paper also considers a case of the beam but with damage in the form of a breathing crack, which induces a nonlinear structural deformation. All previous studies have been done for linear conditions. As future work, we plan to extend our approach to other types of engineering structures including laminated composite plates. The proposed damage indicator is derived on the following.

2.1. The proposed damage indicator. The theory of the strength of materials has provided a set of differential equations describing the dynamics of beam structure when it is subjected to time-varying loads. The so-called Euler-Bernoulli beam theory is accurate to estimate the beam lateral displacement $w(t, x)$ due to dynamic loads $q(t, x)$. The theory relates the both quantities with a fourth-order linear partial differential equation of [32]

$$EI \frac{\partial^4 w(t, x)}{\partial x^4} = -\rho \frac{\partial^2 w(t, x)}{\partial t^2} + q(t, x). \quad (1)$$

The symbol E denotes the beam elastic modulus, I denotes the second moment of area of the beam cross-section, and ρ is the material density.

We should provide notes regarding the underlying assumptions where the governing dynamic was derived. The first is that the magnitude of the lateral deflection $w(t, x)$ is assumed to be very small in comparison to the beam length L . When the deflection is small, the beam cross-section surface remains flat during deformation. For all the time, the cross-section inclines at a right angle with the beam neutral plane.

For structural health monitoring, and for our method to be realizable, we assume that measurement sensors are available where the structural deflection $d(t, x)$ can be obtained within an acceptable level of accuracy. Many instruments, such as laser-based sensors, are available for the purpose. Our proposal is still applicable when the data E , I , ρ , and $q(t, x)$ are unavailable, and for the case, the data $d(t, x)$ taken when the structure is healthy are required.

Based on Equation (1), we propose the following damage indicator $d(t, x)$:

$$d(x, t) = \left| EI \frac{\partial^4 w(t, x)}{\partial x^4} + \rho \frac{\partial^2 w(t, x)}{\partial t^2} - q(t, x) \right|, \quad (2)$$

which simply measures the deviation of the structural dynamics from those of the healthy or intact condition.

The dynamic equilibrium equation is applicable at any point on the beam at any time. We hypothesize that a deviation from the condition may signify a change in either the material properties or the beam geometry or both. Corrosion or crack may alter beam cross-section. Thus, the change may reflect the deterioration in material integrity. Furthermore, we hypothesize when the beam is intact where E , I , and ρ are unaltered, the damage indicator $d(t, x)$ should be zero or very small. The indicator may shift from zero when the beam contains damages. We assume that damages alter the beam deformation $w(t, x)$.

For SHM purposes, we have the freedom to choose the observation or measurement point. We may select the point where the external load is absent ($q(x) = 0$). Thus, it simplifies the computation of the damage indicator.

In this work, we use the Euler-Bernoulli theory not to predict a beam deformation, nor to predict the exerted force, but to estimate the beam integrity. For the purpose, we

propose

$$d(x, t) = \left| EI \frac{\partial^4 w}{\partial x^4} + \rho \frac{\partial^2 w}{\partial t^2} - q(t, x) \right|. \tag{3}$$

In the practical applications, the data E , I , and ρ are potentially unknown to service engineers. In such a case, one may perform a calibration test on the healthy condition to obtain the data $w(t, x)$, and establish a material constant $c = -EI/\rho$ from the relationship:

$$\frac{\partial^4 w(t, x)}{\partial x^4} = c \frac{\partial^2 w(t, x)}{\partial t^2}. \tag{4}$$

The constant is the only parameter required to compute the damage indicator.

The two quantities, namely, $\partial^4 w(t, x)/\partial x^4$ and $\partial^2 w(t, x)/\partial t^2$, are required for the computation of the damage index. In the following section, we describe numerical procedures to establish both.

We also evaluate the index in the frequency domain. For the purpose, we define a time-frequency transformation pair as $u(t) \xleftrightarrow{\text{DFT}} \hat{u}(\omega)$, where DFT stands for the discrete Fourier transform. With the fact that $d^n u(t)/dt^n = (j\omega)^n \hat{u}(\omega)$, and $j^2 = -1$, we obtain the frequency domain damage index, assuming $q(t, x) = 0$:

$$\hat{d}(\omega, x) = EI \frac{\partial^4 \hat{w}(\omega, x)}{\partial x^4} - \rho \omega^2 \hat{w}(\omega, x). \tag{5}$$

2.2. The computation of spatial and time derivatives. Both the quantities $\partial^4 w/\partial x^4$ and $\partial^2 w/\partial t^2$ are obtained numerically. As for the former quantity, we obtain it by the central difference approach.

We compute the term $\partial^4 w/\partial x^4$ by the finite difference approximation of

$$\frac{\partial^4 w(x, t)}{\partial x^4} \approx \frac{w(x - 2h, t) - 4w(x - h, t) + 6w(x, t) - 4w(x + h, t) + w(x + 2h, t)}{h^4}. \tag{6}$$

Thus, $w(t, x)$ should be measured on five adjacent points separated uniformly by a small distance h . In this work, as the required data are established numerically by the finite element method, the length h is taken as the element length, or the distance between two adjacent nodes. We suggest [33] for the readers interested in its derivation and accuracy.

As for the term $\partial^2 w/\partial t^2$, we firstly fit the displacement time-history data with a cubic spline function and then take the first and the second derivatives of the function to provide the acceleration. The derivation of the cubic spline function is as the following.

We consider n data points: $[(t_1, s(t_1)), (t_2, s(t_2)), \dots, (t_n, s(t_n))]$. Strictly, we have the condition: $t_1 < t_2 < \dots < t_n$. We fit the segment in $[t_j, t_{j+1}]$ with a third order polynomial where j is an index from 1 up to n . The polynomial can be written in the Newton form as:

$$p_j(t) = c_{1,j} + c_{2,j}(t - t_j) + c_{3,j}(t - t_j)^2 + c_{4,j}(t - t_j)^3. \tag{7}$$

To complete the polynomial, we should determine the values of the four coefficients: $c_{1,j}$, $c_{2,j}$, $c_{3,j}$, and $c_{4,j}$. They can be computed by

$$c_{1,j} = s(t_j), \tag{8}$$

$$c_{2,j} = m_j, \tag{9}$$

$$c_{3,j} = \frac{[t_j, t_{j+1}]s - m_j}{\Delta t_j} - c_{4,j} \Delta t_j \text{ and} \tag{10}$$

$$c_{4,j} = \frac{m_j + m_{j+1} - 2[t_j, t_{j+1}]s}{(\Delta t_j)^2}. \tag{11}$$

The term m_j denotes the gradient at point t_j . The term $[t_i, \dots, t_{i+k}]s$ denotes the k th divided difference of s at the points t_1, \dots, t_{i+k} . It can be computed by:

$$[t_i, \dots, t_{i+r}]s = \frac{[t_{i+1}, \dots, t_{i+r}]s - [t_i, \dots, t_{i+r-1}]s}{t_{i+1} - t_i}.$$

For given the slopes m_1 at the first point t_1 and m_n at the last point t_n , we can compute the gradients at the points t_2, t_3, \dots, t_{n-1} by solving a set of linear equations:

$$\Delta t_j \cdot m_{j-1} + 2(\Delta t_{j-1} + \Delta t_j) \cdot m_j + \Delta t_{j-1} \cdot m_{j+1} = 3(\Delta t_j [t_{j-1}, t_j]s + \Delta t_{j-1} [t_j, t_{j+1}]s), \quad (12)$$

leading to the gradients m_2, m_3, \dots, m_{n-1} . With these results, we establish the cubic splines for interpolation of the data $w(t, x)$ across the time domain.

2.3. The model of a breathing crack on a beam. Empirical data are required to evaluate the proposed index numerically. For the purpose, we develop a two-dimensional cantilever beam model as shown in Figure 2. This model is adopted from [34], which studied three models of breathing crack for structural health monitoring. With this approach, the empirical data can be quickly generated and used to validate the proposed damage classification method.

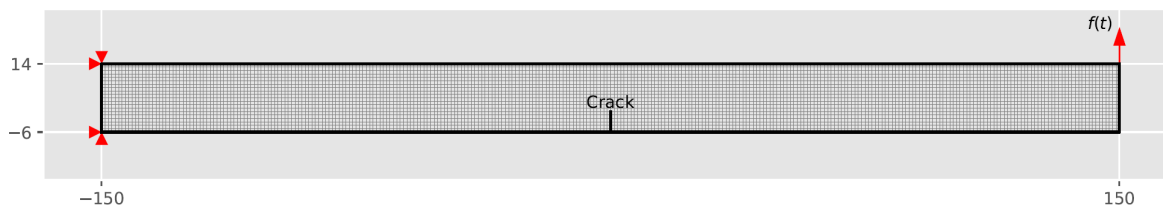


FIGURE 2. The mesh of the finite element model of the 2D beam with a crack. The beam is clamped on its left and its right side is subjected to a harmonic load $f(t)$. For this model, we establish a coordinate system with an origin $(0, 0)$ located at the crack tip.

The beam has a simple geometry and is simply clamped on one of its ends. The beam has a length of 300 mm, a width of 20 mm, and a thickness of 20 mm. In its mid-section, the beam has a crack with a length of 6 mm. The beam is made of steel material. [34] discussed structures made of steel material; however, it did not provide the material data. We also assume that our beam is made of steel material and we assign the following material data: Young's modulus (E) is 207 GPa, Poisson ratio is 0.3, and density (ρ) is 8050 kg/m³. Later, we find our results of the natural frequencies, which will be presented in the next section, are slightly different from those in the reference. We speculate it may be due to a difference in the material data.

The beam is discretized into 6000 square-shape elements. Each element size is 1 mm. The model is built in Ansys, a finite element package, with Ansys's Plane183 element type. The type has eight nodes in rectangular element-shape with quadratic displacement field in each element. Each node has two degrees of freedom: translations in the nodal x and y directions. The finite element model of the beam is shown in Figure 2.

As for the dynamic analysis, from which the model responses are recorded and used for the damage index analysis, the nonlinearity due to the crack is taken into account. On the overlapping nodes on the crack faces, gap elements are built to allow the crack faces interacting in compression only. The element type for the gap elements is Conta178. The model is subjected to a sinusoidal force on the nodes on the model right-end, see Figure 2. The forcing function is at the frequency of 18.153 Hz, about one-tenth of the

natural frequency of the first mode. The analysis is performed for 128 ms. The structural displacements on nodes across the specimen surface are sampled at the rate of 0.5 ms.

The considered beam model allows the occurrence of more complex deformation across the beam thickness than that assumed by the Euler-Bernoulli beam theory. However, with this model, we demonstrate that although the index is derived with a few assumptions about the structural geometry and deformation, it is applicable for more general conditions.

3. Results and Discussion. In this section, we discuss four significant issues related to Structural Health Monitoring (SHM). They are the beam natural frequency, the beam displacement response, the damage indicator in the time domain, and the frequency domain. In particular, we compare the quantities for the cases with and without crack. The first two aspects are traditional in SHM and both are widely used for assessing structural integrity. The last two quantities are the present proposal. We begin with the beam natural frequency.

In Table 1, we present the beam natural frequencies for the first five modes only for the conditions when the beam is healthy and when it contains 6-mm crack. The frequencies are obtained by solving $\det(\mathbf{K} - \omega^2\mathbf{M}) = 0$ for the natural frequency ω where \mathbf{K} is the stiffness matrix and \mathbf{M} is the mass matrix. For the case involving a 6-mm crack, the faces of the crack are assumed separated sufficiently wide such that they are not in contact during the duration of the analysis. The assumption simplifies the model as linear so the natural frequency can be easily obtained.

TABLE 1. The natural frequencies in Hz of the beam with and without crack

Modes	Healthy			Damaged		Change (%) Current
	Current	FE. [34]	Exp. [34]	Current	Exp. [34]	
1	181.5	185.1	185.2	179.0	174.7	1.4
2	1115.0	1159.9	1160.0	1052.9	1155.3	5.6
3	3028.9	3247.6	3245.0	3027.9	3134.8	3.4
4	4229.1			4156.5		1.7
5	5700.4			5453.9		4.3

Also, the table shows the results of the natural frequency provided by Friswell and Penny [34]. They obtained the quantity experimentally and numerically. In this study, we adopt their specimen, which has been utilized by a couple of references, with an expectation that our results can be compared with the existing ones.

It is clear from the table that there are small differences in the natural frequencies between the current model and those in the literature. On the healthy condition, for example, the first three frequencies of the present model are lower by 2.0%, 3.9%, and 6.7%. We speculate the differences are due to material parameters. The reference only stated that their model was made by steel material without providing the exact values of the material properties.

From the above fact, we conclude that the model matches reasonably well with that in the literature. The fact that the difference is getting larger with the mode number should not be an issue as in the dynamic analysis, the beam is subjected with a harmonic load with the frequency of one-tenth of the first natural frequency. Generally, for SHM purposes, only low-frequency vibration is of interest.

As for the natural frequency, what is important for SHM is the change of the frequency due to the crack. In the last column of the table, we obtain the change in percent within

the range of 1.0-6.0. The change is too small to be detectable reliably by the existing methods of modal analysis. We conclude that the use of natural frequency for SHM may not work satisfactorily for the present case.

The second approach of SHM is by observing the change of the deformation pattern. For the purpose, one may quantify the change by a Modal Assurance Criterion (MAC), and other related criteria such as the COordinate Modal Assurance Criterion (COMAC), the Frequency Response Assurance Criterion (FRAC), Coordinate Orthogonality check (ORTHO), Frequency-scaled Modal Assurance Criterion (FMAC), Partial Modal Assurance Criterion (PMAC), and Scaled Modal Assurance Criterion (SMAC).

As for the change of the deformation pattern due to the crack, we show, in Figure 3, the mode shapes for the first five cases, and in Figure 4, we compare the lateral displacements for the beam with and without crack. In general, the change is becoming more visible with time. At the same measurement point, the peak response of the cracked specimen is slightly higher than that without crack. However, the difference is generally very small to be detectable. This remark holds for all measurement points including those where the deformation is small, and those where the deformation is big.

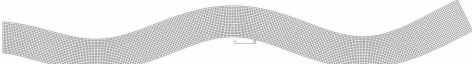
Modes	Healthy	Damaged
1		
2		
3		
4		
5		

FIGURE 3. The first five mode shapes associated with the natural frequencies in Table 1

The third issue we wish to discuss in this section is our proposal for the damage indicator in the time domain. As for the frequency domain, we will discuss it shortly. In the time domain, our proposal is presented in Equation (3). To simplify the computation, we evaluate the index only at some points around the crack where the external load does not exist. With these results, we wish to confirm the previous finding (see [29]) that the index performs well to detect damage when it is computed near the damaged area.

We evaluate the index at the x locations, in mm, of $-50, -40, \dots, 40, 50$. See the center panel of Figure 5. The crack is at $x = 0$. Thus, the evaluation points are evenly distributed around the crack location. Five measurement points are on the left of the crack and five points are on the right of it. The computed damage index is depicted in Figure 5. From the results, we reduce the following notes. The index reaches its higher magnitude when it is evaluated at the closest distance, among the measurement points, to the crack, strengthening the previous remark, which was made based on the case of a simple spring-mass system. The index sensitivity to the crack quickly vanishes with the distance from the crack position. At the measurement point of $x = \pm 10$ mm, the largest

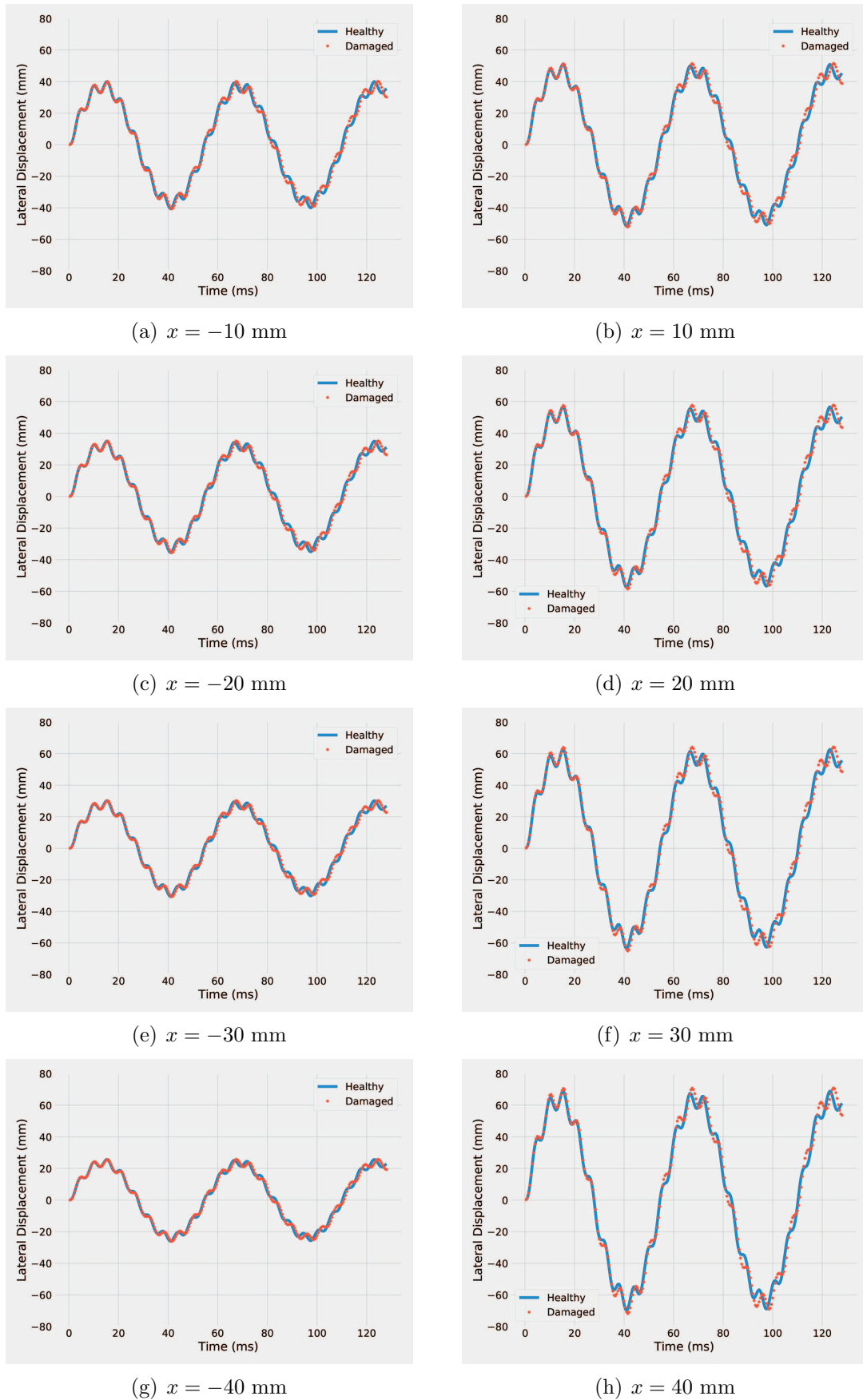


FIGURE 4. The lateral displacement of the beam surface at various locations. The crack is located at $x = 0$.

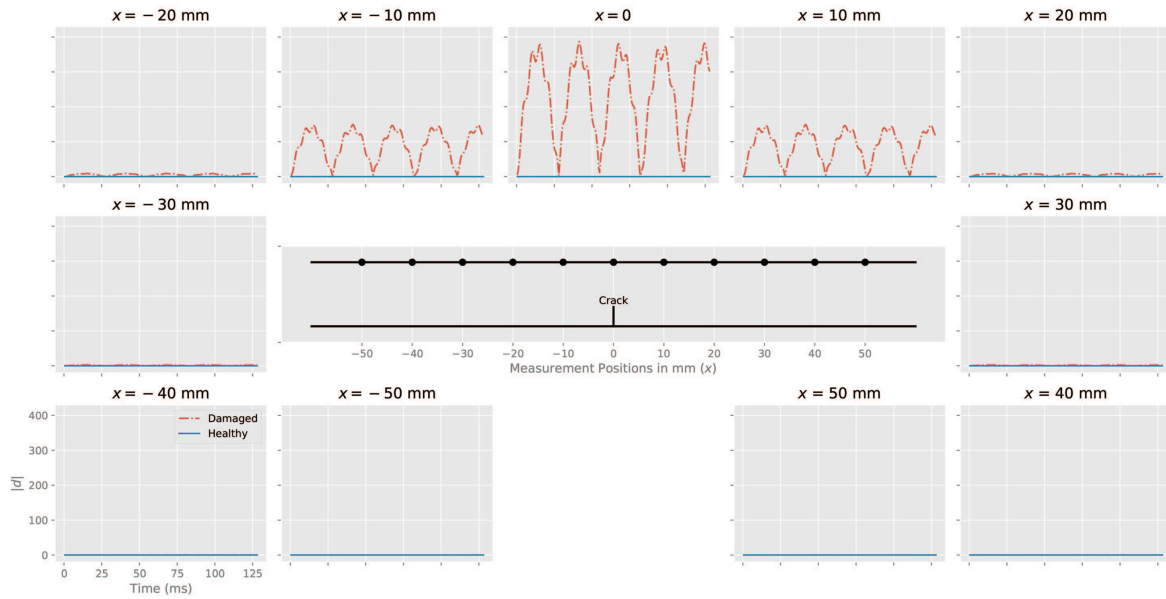


FIGURE 5. The computed time-domain damage index at a number of locations for the beam with and without crack

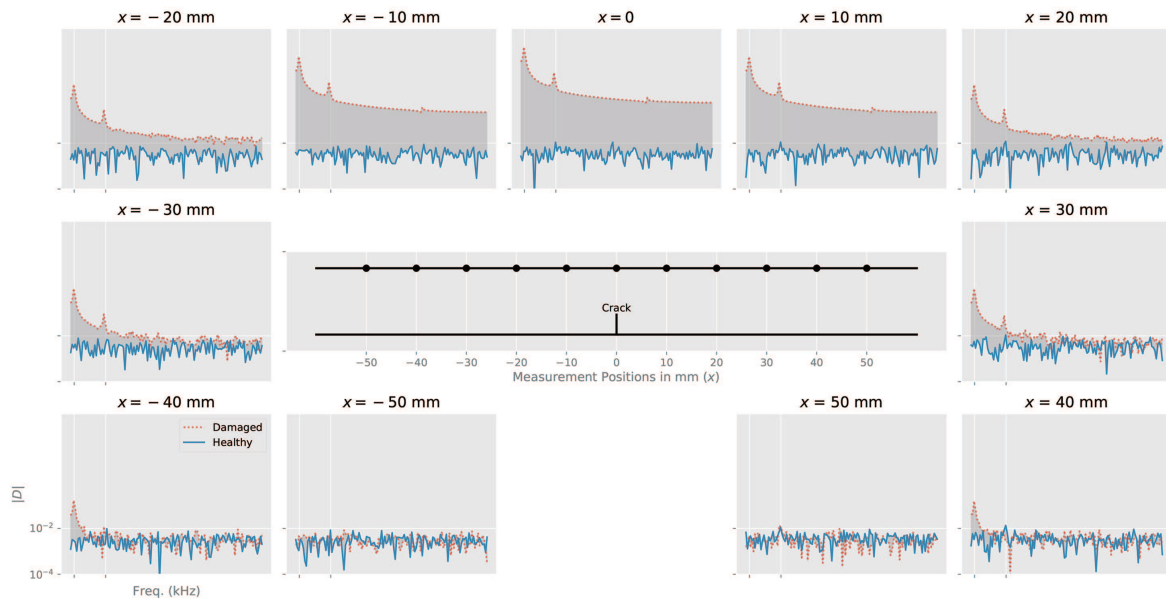


FIGURE 6. The computed frequency-domain damage index at a number of locations for the beam with and without crack. The two vertical grid lines are for the frequency 18.153 Hz and 181.500 Hz.

value of the damage index is only around 40% of the same quantity at the point $x = 0$. Furthermore, at the measurement points $x = \pm 20$ mm, the value of the index has become very small, nearly the same as the case without the crack. Thus, the distance, where the indicator is assessed, to damage is crucial for the current method to detect the damage.

Besides, the results also suggest that the sensitivity of the index to the crack is independent of the scale of the deformation at the point where the quantity is established. The points on the right of the crack undergo much larger deformation than those on the left (see Figure 4). However, the values of the damage index are identical when they are

computed at the same distance from the crack. For example, the figure shows that the values of index at $x = -10$ mm are identical to those at $x = +10$ mm.

The last issue we wish to discuss is about our proposal of the damage index established in the frequency domain. Similar to the previous issue, we also compute the index at those measurement points mentioned above. The index is computed by Equation (5) and the results are depicted in Figure 6.

By comparing these results with those in Figure 5, we conclude that the index is more sensitive in the frequency domain than in the time domain. At $x = 0$, the values of the index for the condition with crack are much higher than those without crack. This pattern is also observable at $x = \pm 10$ mm and $x = \pm 20$ mm. Even on the measurement points as far as $x = \pm 40$ mm, the existence of the crack is still detectable by the index. However, for the case, only the spectra around the load frequency, i.e., at 18.153 Hz, are markedly affected by the crack.

Another interesting result is that for the condition without crack, the damage index is small and random with a constant variance across the considered frequency range. For the case with a crack, the index associated with the load frequency and the first natural frequency is mainly and strongly affected by the crack.

4. Conclusion. In summary, we propose a new approach to monitor the integrity of engineering structures. We propose a damage index derived from our comprehensive and reliable understanding of the structural mechanics of deformation. We have evaluated our proposal for a simple case in [29] and a beam with a smeared damage in [28]. In this paper, we evaluate the proposal on the case involving a breathing crack, which affects the structural deformation in a nonlinear fashion. We evaluate our proposal in both the time and frequency domains and compare its performance with the most widely used method. We find our method is more sensitive to damage than the frequency domain-based method. We note although the natural frequency is less sensitive, it theoretically can monitor damage across the entire part of the structure from a monitoring point. The current method is more sensitive to damage but it only works when the measurement point is around the damage. Besides, we suggest the use of the index in the frequency domain because it is more sensitive and simpler. The index in the time domain can be computed when both displacement and acceleration data are available. In the frequency domain, only displacement data are required. As for future research, we plan to apply the method for various damages in various engineering structures including structures involving composite materials. Besides, the use of better governing dynamics such as Timoshenko theory for beam which takes account of the shear deformation should also be evaluated as it potentially offers a more sensitive damage index. The other potential future research topic is to verify the current method with data collected from a laboratory experiment.

Acknowledgement. This work is supported by Research and Technology Transfer Office, Bina Nusantara University as a part of Bina Nusantara University's International Research Grant entitled "STRUCTURAL HEALTH MONITORING: BEAM WITH BREATHING CRACK CASE" with contract number: No. 026/VR.RTT/IV/2020 and contract date: 6 April 2020.

REFERENCES

- [1] S.-Y. Chu and S.-C. Lo, Application of real-time adaptive identification technique on damage detection and structural health monitoring, *Structural Control Health Monitoring*, vol.16, pp.154-177, 2009.

- [2] E. Caetano, S. Silva and J. Bateira, A vision system for vibration monitoring of civil engineering, *Experimental Techniques*, vol.35, pp.74-82, 2011.
- [3] J. M. W. Brownjohn, A. D. Stefano, Y.-L. Xu, H. Wenzel and A. E. Aktan, Vibration-based monitoring of civil infrastructure: Challenges and successes, *J. Civil Struct. Health Monit.*, vol.1, pp.79-95, 2011.
- [4] T. You, P. Li, Y. Chen and H. Ye, Structural health monitoring of bridge using an adaptive real-time wireless sensor network, *Journal of Convergence Information Technology*, vol.7, no.5, pp.28-35, 2012.
- [5] L. Yu, J.-H. Zhu and L.-L. Yu, Structural damage detection in a truss bridge model using fuzzy clustering and measured FRF data reduced by principal component projection, *Advances in Structural Engineering*, vol.16, no.1, pp.207-217, 2013.
- [6] P. Moser and B. Moaveni, Design and deployment of a continuous monitoring system for the downling hall footbridge, *Experimental Techniques*, vol.37, pp.15-26, 2013.
- [7] A. Cigada, G. Moschioni, M. Vanali and A. Caprioli, The measurement network of the San Siro Meazza stadium in Milan: Origin and implementation of a new data acquisition strategy for structural health monitoring, *Experimental Techniques*, vol.34, pp.70-81, 2009.
- [8] K. Zgonc and J. D. Achenbach, A neural network for crack sizing trained by finite element calculations, *NDT & E International*, vol.29, no.3, pp.147-155, 1996.
- [9] J. R. Mohanty, B. B. Verma, D. R. K. Parhi and P. K. Ray, Application of artificial neural network for predicting fatigue crack propagation life of aluminum alloys, *Archives of Computational Materials Science and Surface Engineering*, vol.1, no.3, pp.133-138, 2009.
- [10] D. Gope, P. C. Gope, A. Thakur and A. Yadav, Application of artificial neural network for predicting crack growth direction in multiple cracks geometry, *Applied Soft Computing*, vol.30, pp.514-528, 2015.
- [11] M. M. Alamdari, T. Rakotoarivelo and N. L. D. Khoa, A spectral-based clustering for structural health monitoring of the Sydney Harbour Bridge, *Mechanical Systems and Signal Processing*, vol.87, pp.384-400, 2017.
- [12] Y.-L. Xu and Y. Xia, *Structural Health Monitoring of Long-Span Suspension Bridge*, Spon Press, 2012.
- [13] M. Mehrjoo, N. Khaji, H. Moharrami and A. Bahreininejad, Damage detection of truss bridge joints using artificial neural networks, *Expert Systems with Applications*, vol.35, no.3, pp.1122-1131, 2008.
- [14] F. L. M. dos Santos, B. Peeters, H. Van der Auweraer, L. C. S. Góes, and W. Desmet, Vibration-based damage detection for a composite helicopter main rotorblade, *Case Studies in Mechanical Systems and Signal Processing*, vol.3, pp.22-27, 2016.
- [15] R. de Medeiros, M. Sartorato, D. Vandepitte and V. Tita, A comparative assessment of different frequency based damage detection in unidirectional composite plates using MFC sensors, *Journal of Sound and Vibration*, vol.383, pp.171-190, 2016.
- [16] M. M. Quinones, L. A. Montejo and S. Jang, Experimental and numerical evaluation of wavelet based damage detection methodologies, *Int. J. Adv. Struct. Eng.*, vol.7, pp.69-80, 2015.
- [17] N. G. Pnevmatikos and G. D. Hatzigeorgiou, Damage detection of framed structures subjected to earthquake excitation using discrete wavelet analysis, *Bulletin of Earthquake Engineering*, vol.15, no.1, pp.227-248, 2017.
- [18] M. Pedram, A. Esfandiari and M. R. Khedmati, Damage detection by a FE model updating method using power spectral density: Numerical and experimental investigation, *Journal of Sound and Vibration*, vol.397, pp.51-76, 2017.
- [19] F. E. Gunawan, Reliability of the power spectral density method in predicting structural integrity, *International Journal of Innovative Computing, Information and Control*, vol.15, no.5, pp.1717-1727, 2019.
- [20] Ch. E. Katsikeros and G. N. Labeas, Development and validation of a strain-based structural health monitoring system, *Mechanical Systems and Signal Processing*, vol.23, no.2, pp.372-383, 2009.
- [21] A. Candelieri, R. Sormani, G. Arosio, I. Giordani and F. Archetti, Assessing structural health of helicopter fuselage panels through artificial neural networks hierarchies, *International Journal of Reliability and Safety*, vol.7, no.3, pp.216-234, 2013.
- [22] A. Candelieri, R. Sormani, G. Arosio, I. Giordani and F. Archetti, A hyper-resolution SVM classification framework: Application to on-line aircraft structural health monitoring, *Procedia – Social and Behavioral Sciences*, vol.108, pp.57-68, 2014.
- [23] M. S. Mhaske and R. S. Shelke, Detection of crack location and depth in a cantilever beam vibration measurement and its comparative validation in ANN and GA, *International Journal of Research in Engineering and Technology*, vol.4, no.10, pp.152-157, 2015.

- [24] F. Archetti, G. Arosio, A. Candelieri, I. Giordani and R. Sormani, Smart data driven maintenance: Improving damage detection and assessment on aerospace structures, *2014 IEEE Metrology for Aerospace (MetroAeroSpace)*, pp.101-106, 2014.
- [25] W. Nick, J. Shelton, K. Asamene and E. Albert, A study of supervised machine learning techniques for structural health monitoring, *Proc. of the 26th Modern AI and Cognitive Science Conference*, Greensboro, NC, USA, vol.1353, pp.133-138, 2015.
- [26] J. Mohanty, B. Verma, P. Ray and D. Parhi, Application of adaptive neuro-fuzzy inference system in modeling fatigue life under interspersed mixed-mode (I and II) spike overload, *Expert Systems with Applications*, vol.38, no.10, pp.12302-12311, 2011.
- [27] J. R. Mohanty, B. B. Verma and P. K. Ray, Prediction of mode-I overload-induced fatigue crack growth rates using neuro-fuzzy approach, *Expert Systems with Applications*, vol.37, no.4, pp.3075-3087, 2010.
- [28] F. E. Gunawan, A new damage indicator for structural health monitoring: Euler-Bernoulli beam case, *ICIC Express Letters, Part B: Applications*, vol.11, no.3, pp.213-220, 2020.
- [29] F. E. Gunawan, The sensitivity of the damage index of the general vibration method to damage level for structural health monitoring, *ICIC Express Letters*, vol.13, no.10, pp.931-939, 2019.
- [30] F. E. Gunawan, B. Soewito, N. Surantha, T. Mauritsius and N. Sekishita, Classification of the structural integrity by the general vibration method, *Procedia Computer Science*, vol.157, pp.382-387, 2019.
- [31] F. E. Gunawan and N. Sekishita, A damage sensitive feature: Beam case, *IOP Conference Series: Materials Science and Engineering*, Jakarta, Indonesia, 2019.
- [32] J. F. Doyle, *Wave Propagation in Structures: An FFT-Based Spectral Analysis Methodology*, Springer-Verlag, New York, 1989.
- [33] J. Kiusalaas, *Numerical Methods in Engineering with Python 3*, Cambridge University Press, 2013.
- [34] M. I. Friswell and J. E. T. Penny, Crack modeling for structural health monitoring, *Structural Health Monitoring*, vol.1, no.2, pp.139-148, 2002.